ZURICH, SWITZERLAND
6 - 10 OCTOBER 2025

EUROPEAN GEOTHERMAL CONGRESS 2025

A geothermal ground source heat pump in an arid climate: first year of operation

Khaled Abdelghafar[1], Francesco Tinti[2], Mohamed Elkarmoty[1], Hany Helal[1], Mohamed Ismael[1]

[1]Cairo University, Faculty of Engineering, Department of Mining, Petroleum, and Metallurgical Engineering, 1 Gamaa Street, 12613, Giza, Egypt

[2] Department of Civil, Chemical, Environmental, and Materials Engineering, University of Bologna, Via Terracini, 28, Bologna, 40131, Italy

khaled.abdelghafar93@cu.edu.eg

Keywords: Ground Source heat Pump, Geothermal for cooling, Arid Climate, Borehole heat exchangers, geothermal potential in Egypt.

ABSTRACT

This study presents an analysis of the energetic, economic, and environmental performance of a ground source heat pump (GSHP) during its initial operational phase in an arid climate in Egypt. The system was implemented as part of the GEB Project, which aims to enhance the capacity of geothermal energy in the country. The installation site experiences extreme climatic conditions, with summer air temperatures exceeding 45°C and minimal precipitation throughout the year, necessitating a thorough evaluation of the system's efficiency and thermal behavior.

As the first shallow geothermal project in Egypt, an experimental borehole heat exchanger (BHE) field was established in the courtyard of the Mining Engineering Department at Cairo University. This field was integrated with a GSHP to provide heating and air conditioning for the 47.25 m^2 seminar room within the rock engineering laboratory. Given the arid climate of Cairo, cooling demand is particularly high, necessitating an in-depth investigation into ground heat dissipation efficiency. Site investigation was carried out to determine the ground thermal properties using different methods. Due to the large amount of injected heat, the ground suffered thermal imbalance. To partially counteract this imbalance, several operating mechanisms were implemented to optimize system performance and adaptability for both scientific research and educational purposes. The installation was equipped with adjustable valves, allowing for flexible switching between parallel, series, and intermediate BHE configurations. This flexibility enables the identification of the most efficient configuration under varying operational conditions, ensuring the system's effectiveness in Egypt's arid climate. Flowing in series, coinciding with the production of DHW during cooling, resulted in the highest efficiency due to the lower circulating water temperatures. Furthermore, the series flow resulted in the highest efficiency during heating activity.

1. INTRODUCTION

Using shallow geothermal energy for cooling in an arid climate, such as the Middle East countries, especially in Egypt, is not widely investigated. Few publications focused on it, as most of the published work is concentrated in the developed countries, where heating demand is dominant [1]. In Egypt, there is no published use for geothermal energy except for medical purposes, using the hot springs [2]. Due to the fossil fuel crisis and environmental restrictions, Egypt aims to increase the share of renewable energy in power production to 42% by 2035 [3]. Shallow geothermal energy was investigated for the first time in the country within the framework of an Erasmus+ funded project "GEB" by installing a pilot plant for cooling at Cairo University. The ground characteristics for utilizing shallow geothermal energy were collected in this study, with an undisturbed ground temperature (UGT) of 24.10 °C and 25.10 °C, using different methods of determination [4]. In Saudi Arabia, UGT reached 32.50 °C, which, however, being high, showed reasonable cooling potential [5]. Several studies from Saudi Arabia have been conducted, utilizing numerical simulation and design calculations, which have shown higher efficiency for the ground source heat pump (GSHP) compared to the air source heat pump (ASHP) [6,[6]. Moreover, numerical modelling based on the ground temperature obtained through the empirical equation of Kusuda confirmed the high efficiency of GSHP in Morocco [7]. In the United Arab Emirates (UAE), measurements showed an UGT of 32.40 °C. An experimental setup of horizontal pipes buried 2.50 m deep and connected to a circulation pump with heaters showed ground saturation after a short period [1]. Around 8 projects were installed in Jordan, where the ground temperature reached 22 °C. The first period of operation showed that the systems covered the heating and cooling loads [8]. All the reviewed cases in countries near Egypt showed higher efficiency of GSHP. This outperformance did not encourage the widespread use of the GSHP due to the high capital costs and the thermal imbalance resulting from the high cooling demand. Integration with solar systems or cooling towers to reduce the ground-injected heat was

proposed. In Egypt, where cooling loads are significantly high, a pilot borehole heat exchanger (BHE) system was designed and installed to assess optimal solutions for mitigating ground thermal imbalance. The system was equipped with appropriate valves to enable switching between parallel and series flow arrangements, as well as different BHE designs, including single-U and double-U pipe configurations. This experimental setup aims to evaluate the most effective configuration for enhancing thermal performance and long-term system stability.

2. SITE CHARACTERISTICS

At Cairo University, the ground characteristics at the site were investigated through two methods. The first method included drilling, collecting, and testing samples from an exploration borehole equipped as a piezometer, in addition to the temperature measurement inside this borehole throughout the year using a phreatimeter borehole ground temperature (**Fig. 1**) to obtain the ground temperature profile versus depth (**Fig. 2**). Secondly, thermal response tests (TRTs) were carried out on 3 different borehole heat exchangers (BHEs) to get the ground thermal properties for the first time in Egypt (**Fig. 3**). The line source model was applied to interpret the TRT data [9] using equations [1,2]. The ground thermal conductivity was obtained at the 3 BHEs by getting the slope of the borehole average temperature on a logarithmic scale (**Fig. 4**).

Figure 1: Measuring ground temperature in the piezometer during the exploration stage.

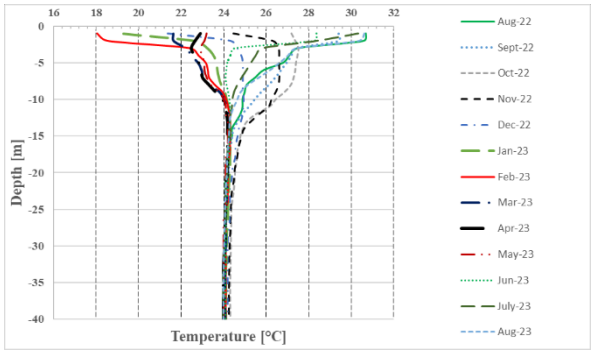

Figure 2: Ground temperature profile along the exploration borehole depth [4].

$$T(t) = m \cdot \ln(t) + b \qquad [1]$$

$$m = \frac{1}{4 \cdot \pi \cdot \lambda} \qquad [2]$$

Figure 3: Carrying out onsite thermal response test on BHE-2.

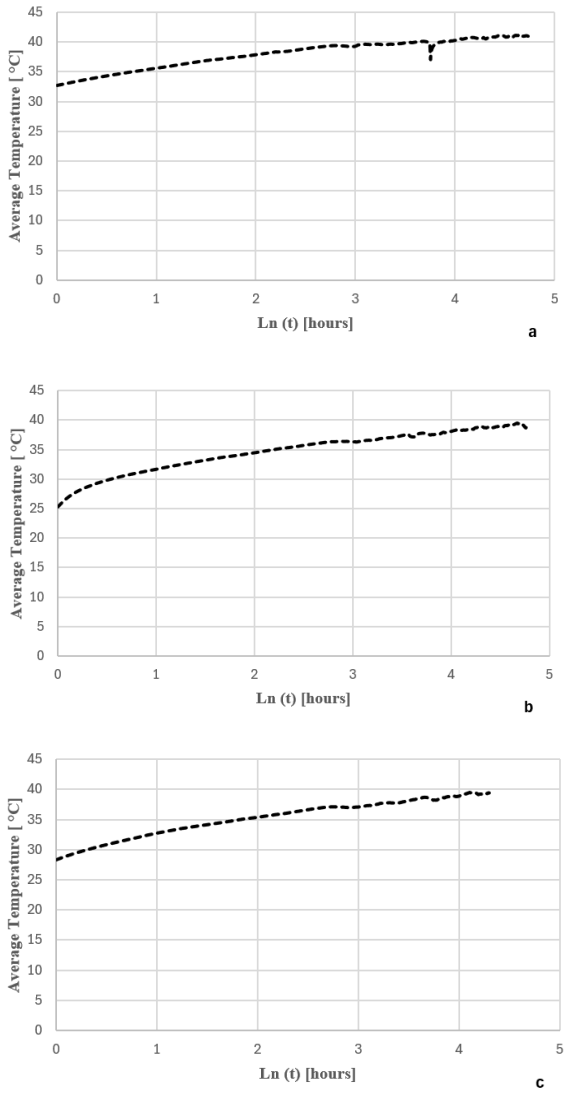

Figure 4: Average temperature versus natural logarithm of time - TRT interpretation for a) BHE-1, b) BHE-2, c) BHE-3.

An average UGT of 25.10 °C resulted from the TRT, which is 4.15 % higher than the one measured in the piezometer.

The results of the ground thermal conductivity showed a higher variation of 2.10 W/m.°C from the first method

(**Fig. 5**) compared to 2.53 W/m.°C resulting from the TRT method. These values are attributed to the existence of sand along the borehole depth, which is mainly composed of sand and clay. According to fixed temperature sensors at Cairo University's Climate Control Unit, the maximum air temperature reaches 46 °C during summer, which indicates a high cooling demand. The higher difference between the air and ground temperatures encouraged the implementation of the pilot plant.

On the other hand, the groundwater level is shallow in the study area, around 2 m below the ground surface. The existence of the groundwater represents an advantage for higher heat exchange between the ground and the pipes.

3. DESIGN AND INSTALLATION OF THE GEOTHERMAL PILOT PLANT

Based on in-situ data collection, a geothermal pilot plant was designed and implemented to provide cooling for a seminar room within the Rock Engineering Laboratory (REL) at the Faculty of Engineering, Cairo University. The design was conducted using Earth Energy Design (EED) software to optimize the system's configuration and performance parameters before implementation. The system comprises three borehole heat exchangers (BHEs) with a total depth of 120 m, connected to a 9-kW ground source heat pump (GSHP) manufactured by Ecoforest Co. The BHE field consists of two single-U BHEs and one double-U BHE (**Fig. 6)**. High-density polyethylene (HDPE) pipes with a diameter of 32 mm were installed within the boreholes and connected to the heat pump via horizontally buried pipes (50 mm in diameter) at a depth of 1 m. To ensure system integrity, all piping connections were tested for leakage and subsequently thermally insulated. The two legs of each BHE were spaced 50 mm apart using fixed spacers positioned at regular intervals along the pipe length.

The borehole annulus was filled with a locally sourced grout, selected after testing the thermal conductivity of various grouting materials, with the chosen grout exhibiting the highest thermal conductivity of 2.55 W/m·°C. Appropriate valve configurations were incorporated to regulate flow dynamics and allow switching between parallel and series flow arrangements.

Additionally, buffer tanks were installed between the heat pump and the indoor fan coil units, with power consumption around 100 W each, to maintain stable system performance. A 200 L domestic hot water (DHW) tank was also integrated into the GSHP system to utilize the rejected heat for hot water production (**Fig. 7**). The primary objectives of this geothermal system are to provide space cooling, heating, and domestic hot water.

Figure 5: A sample collected from a drilled borehole for laboratory testing.

Figure 6: Drilling of the borehole heat exchanger field.

Figure 7: GSHP system installed at Cairo University.

4. MITIGATION STRATEGIES FOR THE GROUND THERMAL IMBALANCE

Several operational strategies were implemented to mitigate the impact of continuous heat injection during the cooling season in summer. Heat extraction was achieved through space heating in winter and the production of DHW to counteract the increase in the ground temperature. Additionally, the system was alternated between parallel and series flow

configurations to assess their effects on overall efficiency under two different flow rates. Furthermore, the performance of single U-tube and double U-tube pipe configurations was analyzed. The influence of the groundwater flow direction on heat dissipation was also examined.

The system started operating in cooling mode at the end of August 2024, while the water temperature was recorded at the inlet and outlet for both the BHEs and the heat pump. Multiple system configurations were tested to evaluate the efficiency of all operating modes described in **Table 1**, including both parallel and series flow arrangements, with and without domestic hot water (DHW) production. To achieve the high flow rate configuration, an additional external 1-hp circulation pump was installed to increase the brine circuit's water flow. For the low flow rate mode, the internal circulation pump of the ground source heat pump (GSHP) was used. During the efficiency tests, Permutations and combinations were applied to work using only two BHEs rather than three. Two Single U BHEs were used during that time, while the third one, which is the double U BHE, was blocked. Furthermore, only one single U and one double U BHEs were used, while the third one, "single U", was blocked.

The system's operating modes were tested separately over several working days. The system's performance during each working day is listed in the **Tables below.**

The average power consumption of GSHP (P_{HP}) and cooling system output (P_{Cool}) during operation were recorded in KW to evaluate efficiency based on the energy efficiency ratio (EER) across all operating scenarios. See equation [3].

$$EER = \frac{P_{Cool}}{P_{HP}} \qquad [3]$$

5. RESULTS AND DISCUSSION

The borehole inlet and outlet water temperatures had been recorded at the top of the BHEs during all operating modes. The whole cooling season duration was divided into several periods in which different operating modes with several BHE configurations were applied. The first weeks had experienced several trials to ensure the system's reliability.

Table 2. shows the performance results of the first period at the end of August, having the water circulating in a parallel manner. A noticeable decrease in water temperature was observed on August 29th during the domestic hot water (DHW) production phase, despite temperatures previously exceeding 43 °C, as illustrated in **Fig. 8.**

Table 1: Description of system configurations

System mode	Configuration details
P-L-DHW	Parallel – low flow- With DHW production
P-L-No DHW	Parallel – low flow- without DHW production
P-H-DHW	Parallel – High flow- With DHW production
P-H-No DHW	Parallel – High flow- without DHW production
S-L-DHW	Series – low flow- With DHW production
S-L-No DHW	Series – low flow- without DHW production
S-H-DHW	Series – High flow- With DHW production
S-H-No DHW	Series – High flow- without DHW production
2 S-L-DHW	Two single U- Low Flow- With DHW production
2 S-L-No DHW	Two single U- Low Flow- Without DHW production
2 S-H-DHW	Two single U-High Flow- With DHW production
2 S-H-No DHW	Two single U-High Flow- Without DHW production
1S+1D-L-DHW	One Single U and one Double U- Low Flow- With DHW production
1S+1D-L-No DHW	One Single U and one Double U- Low Flow- Without DHW production
1S+1D-H-DHW	One Single U and one Double U- High Flow- With DHW production
1S+1D-H-No DHW	One Single U and one Double U- High Flow- Without DHW production

Table 2: Operation scheduling during cooling mode- Period 1

Period (1) 26 Aug – 1 Sept 2024				
Date	**Mode**	**P_{HP} (KW)**	**P_{Cool} (KW)**	**EER**
26 Aug 2024	P-L-No DHW	2.60	7.50	2.88
29 Aug 2024	P-L-DHW	2.40	7.10	2.96
1 Sept 2024	P-L-DHW	2.20	6.60	3.00

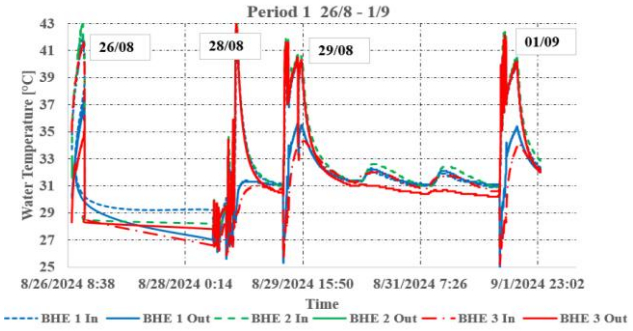

Figure 8: Inlet and outlet water temperatures at BHEs – Period 1

After that, the series flow rate was tested in the second period at the beginning of September, applying the low flow rate conditions. The whole period included the application of DHW at the early hours of operation until reaching the hot water set temperature. **Table 3**. Shows examples from this period. Water temperatures recorded throughout the whole period are shown in **Fig.9**. The system recorded a peak borehole entering water temperature of 45 °C on September 4th and 5th, coinciding with an operational day utilizing the serial flow arrangement. This temperature increase followed a temporary stop in DHW production, triggered by reaching the hot water temperature setpoint. The simultaneous operation of DHW production and space cooling was found to mitigate the rise in water temperature.

Table 3: Operation scheduling during cooling mode-Period 2

Period (2) 2 Sept – 9 Sept 2024				
Date	**Mode**	**P_{HP} (KW)**	**P_{Cool} (KW)**	**EER**
5 Sept 2024	S-L-DHW	3.10	7.50	2.42
8 Sept 2024	S-L-DHW	2.20	7.00	3.18

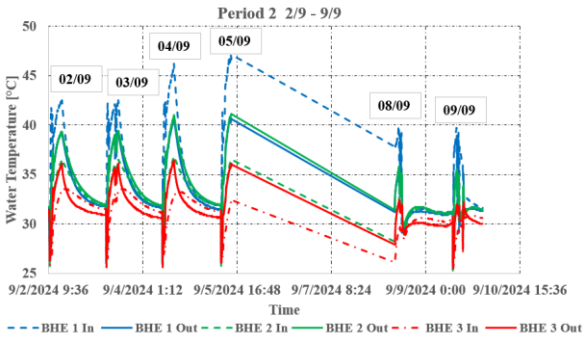

Figure 9: Inlet and outlet water temperatures at BHEs – Period 2

The third period, listed in **Table 4**, included one of the highest efficiency scenarios (S-H-DHW) with an EER = 3.40. After that, one of the BHEs was blocked. Working with a double u BHE besides a single u resulted in higher efficiency than the two single u BHEs. **Fig.10** demonstrates an initial drop in water temperature on the first day of this operational period, attributed to a higher flow rate and the serial flow. This was followed by a gradual increase in temperature, resulting from the deactivation of one BHE, which led to reliance on the remaining BHEs with shorter lengths

Table 4: Operation scheduling during cooling mode-Period 3

Period (3) 10 Sept – 17 Sept 2024				
Date	**Mode**	**P_{HP} (KW)**	**P_{Cool} (KW)**	**EER**
11 Sept 2024	S-H-DHW	2.00	6.80	3.40
12 Sept 2024	2 S-L-DHW	2.50	7.70	3.08
16 Sept 2024	2 S-H-No DHW	2.80	7.90	2.82
17 Sept 2024	1 S +1 D - H-No DHW	2.40	7.00	2.92

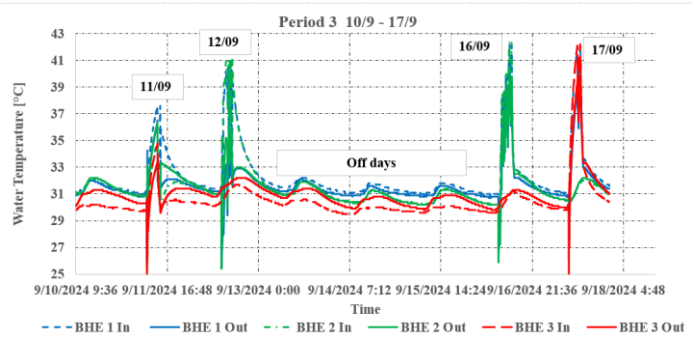

Figure 10: Inlet and outlet water temperatures at BHEs – Period 3

The influence of flow rate is further evidenced in **Fig. 11**, which compares the last two days of operation during the fourth period listed in **Table 5**.

Fig. 12 reinforces these findings by comparing system performance on September 29th and 30th. The results show a higher water temperature on September 29th, when DHW was not produced, compared to September 30th, when DHW production was active. Moreover, the higher flow rate reduced the water temperature and subsequently increased the efficiency by comparing the first two days of the fifth period listed in **Table 6**. Combining both effects, having the system working in series using a higher flow rate while producing DHW, resulted in the highest efficiency during this period.

Table 5: Operation scheduling during cooling mode-Period 4

Period (4) 18 Sept – 23 Sept 2024				
Date	**Mode**	**P_{HP} (KW)**	**P_{Cool} (KW)**	**EER**
18 Sept 2024	1 S +1 D -L-No DHW	2.40	7.00	2.92
22 Sept 2024	P-H-No DHW	2.00	6.80	3.40
23 Sept 2024	P-L-No DHW	2.00	6.70	3.35

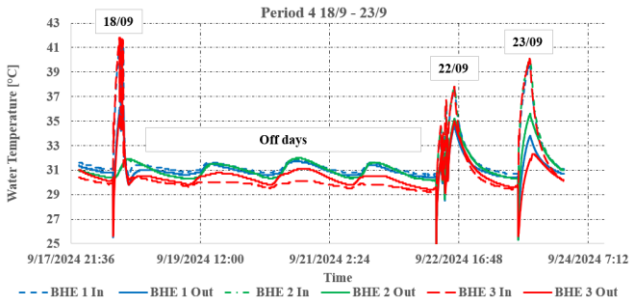

Figure 11: Inlet and outlet water temperatures at BHEs – Period 4

Table 6: Operation scheduling during cooling mode-Period 5

Period (5) 24 Sept – 2 Oct 2024				
Date	Mode	P_{HP} (KW)	P_{Cool} (KW)	EER
24 Sept 2024	P-L-DHW	2.00	6.80	3.40
25 Sept 2024	P-H-DHW	1.60	6.10	3.81
29 Sept 2024	S-L-No DHW	2.10	6.70	3.19
30 Sept 2024	S-L-DHW	2.00	6.50	3.25
1 Oct 2024	S-H-No DHW	1.70	6.00	3.53
2 Oct 2024	S-H-DHW	1.60	6.00	3.75

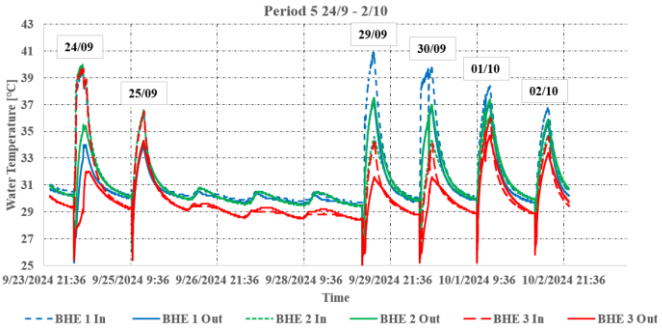

Figure 12: Inlet and outlet water temperatures at BHEs – Period 5

This trend is further confirmed in **Fig. 13**, which compares the first two days of measurements within the sixth period listed in **Table 7** and highlights the impact of the flow rate on the performance.

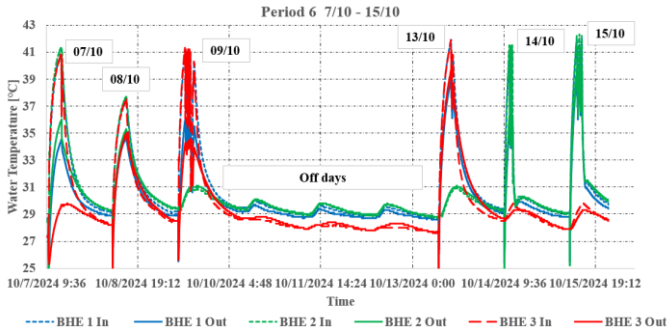

Figure 13: Inlet and outlet water temperatures at BHEs – Period 6

Table 7: Operation scheduling during cooling mode-Period 6

Period (6) 7 Oct – 15 Oct 2024				
Date	**Mode**	**P_{HP} (KW)**	**P_{Cool} (KW)**	**EER**
7 Oct 2024	P-L-No DHW	2.00	6.20	3.10
8 Oct 2024	P-H-No DHW	1.70	6.10	3.59
9 Oct 2024	1 S +1 D -L-No DHW	2.00	6.50	3.25
13 Oct 2024	1 S +1 D -H-No DHW	2.00	6.30	3.15
14 Oct 2024	2 S-L-No DHW	2.10	6.60	3.14
15 Oct 2024	2 S-H-No DHW	2.00	6.30	3.15

Fig. 14 emphasizes the combined effects of flow rate and DHW production during the seventh period of operation, as listed in **Table 8**. This period presented

the results already stated in the previous periods of operation.

Table 8: Operation scheduling during cooling mode-Period 7

Period (7) 17 Oct – 27 Oct 2024				
Date	**Mode**	**P_{HP} (KW)**	**P_{Cool} (KW)**	**EER**
17 Oct 2024	S-L-No DHW	1.90	6.00	3.16
20 Oct 2024	S-H-No DHW	1.60	5.85	3.66
22 Oct 2024	S-L-DHW	1.60	5.90	3.69
23 Oct 2024	S-H-DHW	1.10	5.40	4.91
27 Oct 2024	S-L-DHW	1.80	5.80	3.22

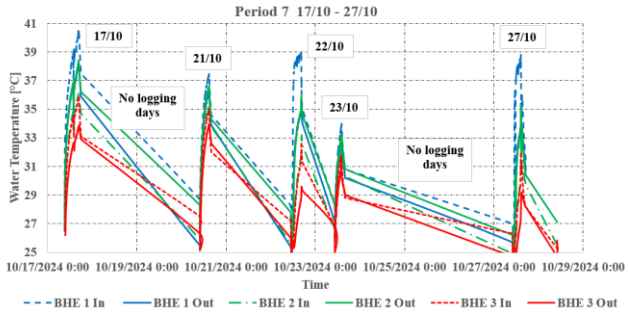

Figure 14: Inlet and outlet water temperatures at BHEs – Period 7

Fig. 15 presents temperature measurements recorded during the final stage of the cooling season. According to the temperature measurements at BHEs and the results presented in **Table 9**, the combined effect of the serial flow associated with the high flow rate in the presence of DHW production showed the highest efficiency and the lowest borehole water temperatures. Using an ultrasonic flow meter, the flow encountered a higher pressure drop, which decreased the flow rate and enhanced the temperature difference between the borehole inlet and outlet water temperatures. Subsequently, the system consumed higher power to overcome the higher resistance. Overall, the operating mode influenced the power consumption of GSHP. Applying DHW and using a series flow arrangement reduced power consumption for many days due to the lower borehole outlet water temperature.

Table 9: Operation scheduling during cooling mode-Period 8

Period (8) 28 Oct – 5 Nov 2024				
Date	**Mode**	**P_{HP} (KW)**	**P_{Cool} (KW)**	**EER**
28 Oct 2024	S-L-DHW	1.50	5.20	3.47
29 Oct 2024	S-H-DHW	1.20	5.00	4.17
30 Oct 2024	S-H-DHW	1.10	5.00	4.55
3 Nov 2024	S-L-DHW	1.20	4.70	3.92
5 Nov 2024	P-H-DHW	1.00	4.70	4.70

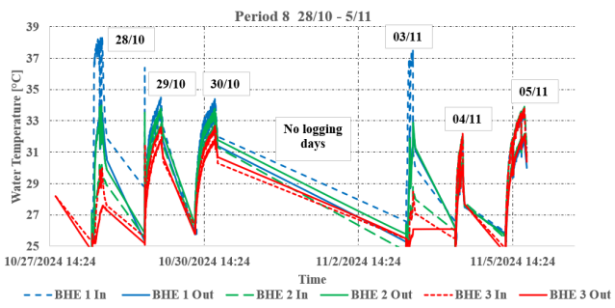

Figure 15: Inlet and outlet water temperatures at BHEs – Period 8

On the other hand, heating during winter did not benefit from the free production of DHW due to the increased power consumption during the hot water production phase. When employing the series flow, lower inlet and outlet temperatures were observed. Consequently, a higher water temperature was observed in the distribution system. The average power consumption of GSHP (P_{HP}), heating system output (P_{Heat}), and system's efficiency in terms of coefficient of performance (COP), shown in equation 4, were recorded and listed in **Table 10** for the selected working days representing several operating configurations. Parallel and series flow were tested during the heating activity, with and without DHW production, all depending on the internal circulation pump (low flow rate conditions). **Fig. 16** presents inlet and outlet temperatures recorded during a day when the system was configured as a series flow. The performance of the system was affected due to the stop in hot water production once the hot water set temperature was reached. The series flow arrangement had the highest efficiency for the GSHP when the production of DHW was not in use.

$$COP = \frac{P_{Heat}}{P_{HP}} \quad [4]$$

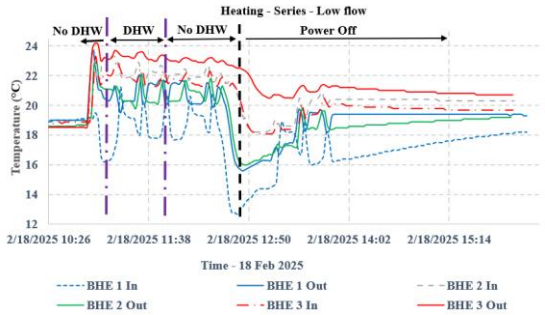

Figure 16: Inlet and outlet water temperatures at BHEs – heating mode

Finally, during the first year of operation for the geothermal system, including summer and winter seasons in Egypt's climate, the system demonstrated greater efficiency during the heating season compared to the cooling season. The coefficient of performance (COP) of the GSHP for heating ranged from 4.81 to 13.33 with an average value of 6.24. In contrast, the energy efficiency ratio (EER) during cooling mode ranged from 2.42 to 4.91 for the GSHP, as shown in **Fig.17**.

Table 10: Operation scheduling during heating mode

Date	Operating mode	P_{HP} (KW)	P_{Heat} (KW)	COP
5 Feb 2025	P-L-No DHW	1.35	6.50	4.81
9 Feb 2025	P-L-No DHW	1.2	6.80	5.67
12 Feb 2025	S-L-No DHW	1.10	6.50	5.91
13 Feb 2025	S-L-No DHW	1.20	6.35	5.29
13 Feb 2025	S-L-No DHW	0.85	5.00	5.88
18 Feb 2025	S-L-No DHW	0.45	6.00	13.33
18 Feb 2025	S-L-DHW	2.70	14.00	5.19
25 Feb 2025	P-L-No DHW	1.10	6.20	5.64
26 Feb 2025	P-L-DHW	2.60	14.00	5.38
26 Feb 2025	P-L-No DHW	1.00	5.30	5.30

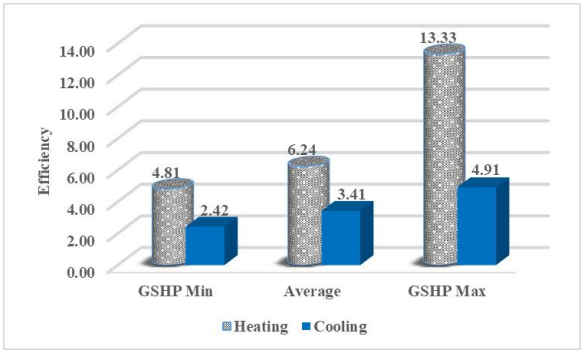

Figure 17: GSHP efficiency for both heating and cooling at Cairo University project

6. CONCLUSIONS

The main findings of this study can be summarized as follows:

- Implementing a series flow configuration through the borehole heat exchangers (BHEs) effectively mitigated the rise in water temperature, thereby enhancing the overall system efficiency.
- The integration of domestic hot water (DHW) production contributed to a reduction in both inlet and outlet borehole temperatures, which in turn improved system performance.
- The highest energy efficiency ratio (EER) values were achieved under the simultaneous space cooling and domestic hot water (S-H-DHW) operating mode, particularly when employing a series flow configuration with a high flow rate and active hot water production.
- Geothermal energy demonstrates significant potential for both heating and cooling applications in Egypt.
- The ground source heat pump (GSHP) system exhibited greater efficiency in heating mode than in cooling mode, attributed to Egypt's relatively high ground temperatures and modest heating demands.
- During the heating operation, the GSHP achieved a COP ranging from 4.81 to 13.33.
- During the cooling operation, the GSHP recorded EER values ranging from 2.42 to 4.91.
- The production of hot water alongside cooling is nearly free; however, it requires a considerable increase in power consumption during the heating mode.
- The series flow arrangement achieved the highest efficiencies for both heating and cooling. Associated with DHW production in the cooling mode, and without DHW production for the heating mode.
- Using heating during the winter season reduces the circulated water temperature and therefore can suppress the ground temperature increase.

REFERENCES

[1] H. Atwany, M. O. Hamdan, B. A. Abu-nabah, and A. Hai, "Experimental evaluation of ground heat exchanger in UAE." *Renew Energy*, vol. 159, pp. 538–546, 2020, doi: 10.1016/j.renene.2020.06.073.

[2] J. W. Lund and A. N. Toth, "Direct utilization of geothermal energy 2020 worldwide review." *Geothermics*, vol. 90, no. November 2020, 2021, doi: 10.1016/j.geothermics.2020.101915.

[3] S. I. Salah, M. Eltaweel, and C. Abeykoon, "Towards a sustainable energy future for Egypt: A systematic review of renewable energy sources, technologies, challenges, and recommendations." *Clean Eng Technol*, vol. 8, no. December 2021, p. 100497, 2022, doi: 10.1016/j.clet.2022.100497.

[4] K. Abdelghafar, F. Tinti, M. Ismael, H. Helal, and M. Elkarmoty, "A pilot borehole heat exchanger field in Egypt: Subsoil investigation, thermal response tests and sensitivity analysis." *Geothermics*, vol. 127, p. 103241, Mar. 2025, doi: 10.1016/j.geothermics.2024.103241.

[5] M. H. Sharqawy, S. A. Said, E. M. Mokheimer, M. A. Habib, H. M. Badr, and N. A. Al-shayea, "First in situ determination of the ground thermal conductivity for borehole heat exchanger applications in Saudi Arabia." *Renew Energy*, vol. 34, no. 10, pp. 2218–2223, 2009, doi: 10.1016/j.renene.2009.03.003.

[6] F. Alshehri, S. Beck, D. Ingham, L. Ma, and M. Pourkashanian, "Techno-economic analysis of ground and air source heat pumps in hot dry climates." *Journal of Building Engineering*, 2019.

[7] M. Ougazzou, A. El Maakoul, I. Khay, A. Degiovanni, and M. Bakhouya, "Techno-economic and environmental analysis of a ground source heat pump for heating and cooling in Moroccan climate regions." *Energy Convers Manag*, vol. 304, Mar. 2024, doi: 10.1016/j.enconman.2024.118250.

[8] S. Al-Zyoud, "Geothermal Energy Utilization in Jordanian Deserts." *International Journal of Geosciences*, vol. 10, no. 10, pp. 906–918, 2019, doi: 10.4236/ijg.2019.1010051.

[9] S. Mohammadzadeh Bina, H. Fujii, D. Qaisova, R. Lein, J. Rahmatov, and F. Inagaki, "Ground source heat pump systems in Central Asia: A case study from Dushanbe, Tajikistan." *Geothermics*, vol. 128, May 2025, doi: 10.1016/j.geothermics.2025.103281.

Acknowledgements

The authors would like to express their sincere gratitude to the GEB Project and the Erasmus+ Program for their financial support in the construction of the first shallow geothermal pilot plant in Egypt. Special thanks are also extended to the project partners for their valuable contributions and continuous support. Additionally, the authors acknowledge United Group Co. for its outstanding execution of the project, marking a significant milestone as the first of its kind in Egypt.